Development 135, 2065-2070 (2008) doi:10.1242/dev.022673

Cell cycle progression is required for zebrafish somite morphogenesis but not segmentation clock function

Lixia Zhang, Christina Kendrick, Dörthe Jülich and Scott A. Holley*

Cell division, differentiation and morphogenesis are coordinated during embryonic development, and frequently are in disarray in pathologies such as cancer. Here, we present a zebrafish mutant that ceases mitosis at the beginning of gastrulation, but that undergoes axis elongation and develops blood, muscle and a beating heart. We identify the mutation as being in *early mitotic inhibitor 1* (*emi1*), a negative regulator of the Anaphase Promoting Complex, and use the mutant to examine the role of the cell cycle in somitogenesis. The mutant phenotype indicates that axis elongation during the segmentation period is driven substantially by cell migration. We find that the segmentation clock, which regulates somitogenesis, functions normally in the absence of cell cycle progression, and observe that mitosis is a modest source of noise for the clock. Somite morphogenesis involves the epithelialization of the somite border cells around a core of mesenchyme. As in wild-type embryos, somite boundary cells are polarized along a Fibronectin matrix in *emi1*$^{-/-}$. The mutants also display evidence of segment polarity. However, in the absence of a normal cell cycle, somites appear to hyper-epithelialize, as the internal mesenchymal cells exit the core of the somite after initial boundary formation. Thus, cell cycle progression is not required during the segmentation period for segmentation clock function but is necessary for the normal segmental arrangement of epithelial borders and internal mesenchymal cells.

KEY WORDS: Somitogenesis, Cell cycle, Zebrafish, *emi1*, Somite morphogenesis

INTRODUCTION

Somites are the segmented precursors to the axial skeleton and musculature created as the trunk and tail elongate. The periodic formation of somites is governed by the segmentation clock, which creates oscillations in gene expression in the presomitic mesoderm (PSM) (Pourquié, 2003). In zebrafish, the segmentation clock requires Notch signaling, while the amniote clocks also incorporate Wnt and Fgf signaling (Holley, 2007). It is debated whether the Notch, Wnt or Fgf pathways constitute core components of the clock, or whether they are a readout of a global clock that governs all of embryonic development (Aulehla et al., 2003; Dequeant et al., 2006; Niwa et al., 2007; Wahl et al., 2007). For instance, some models link the segmentation clock to the cell cycle oscillator (Collier et al., 2000; McInerney et al., 2004; Primmett et al., 1989; Primmett et al., 1988).

Somite morphogenesis occurs as the segment boundary cells undergo a mesenchymal to epithelial transition (MET), forming a ball of cells with an epithelial surface and a core of mesenchyme (Holley, 2007). Zebrafish somite morphogenesis requires the transcription factor *fused somites* (*fss*; also known as *tbx24*), Eph/Ephrin signaling and *integrin α5*/*fibronectin* function (Barrios et al., 2003; Durbin et al., 1998; Durbin et al., 2000; Jülich et al., 2005a; Koshida et al., 2005; Nikaido et al., 2002; van Eeden et al., 1996). *fss* links the segmentation clock and somite morphogenesis (Holley et al., 2000). *fss* mutants fail to maintain the segmentation clock in the anterior PSM, lack segment polarity and *ephA4* (*epha4a* – Zebrafish Information Network) expression, and exhibit a complete loss of MET in the paraxial (somitic) mesoderm (Durbin et al., 2000; Holley et al., 2000; Oates et al., 2005b; van Eeden et al., 1998). However, exogenous expression of *ephA4* in genetic mosaics can induce boundaries in *fss*$^{-/-}$ embryos (Barrios et al., 2003). Similarly in mouse genetic mosaics, EphA4 expression correlates with boundary formation (Nakajima et al., 2006). Integrin α5-GFP clusters along the basal side of nascent somite boundary cells, and *integrin α5* and its ligand *fibronectin* are required for the maintenance and full maturation of the boundary in zebrafish, mice and *Xenopus* (Georges-Labouesse et al., 1996; Goh et al., 1997; Jülich et al., 2005a; Koshida et al., 2005; Kragtorp and Miller, 2007; Yang et al., 1993). Double mutants between *integrin α5* and the Notch pathway lead to a complete loss of MET in the paraxial mesoderm (Jülich et al., 2005a). Simultaneous loss of *ephrin B2a*, a ligand for *ephA4*, and *integrin α5* leads to a synergistic defect in somite boundary morphogenesis (Koshida et al., 2005). Ena/Vasp and Fak, which function in Integrin signaling, are necessary for somite formation in *Xenopus* (Kragtorp and Miller, 2006). Chick somite morphogenesis is regulated by Snail2 and Cdc42, which promote mesenchymal cell morphology, and Rac1, which fosters epithelial cell morphology (Dale et al., 2006; Nakaya et al., 2004).

Emi1 is a negative regulator of the Anaphase Promoting Complex (APC) and is required for entry into mitosis in *Xenopus* embryos (Reimann et al., 2001). APC, an E3 ubiquitin ligase, also functions in post-mitotic cells. In *Drosophila* and *C. elegans* neurons, APC localizes to the synapse and regulates the turnover of glutamate receptors (Juo and Kaplan, 2004; van Roessel et al., 2004). In vertebrate neurons, inhibition of APC by RNA interference or overexpression of Emi1 increases axonal growth and overcomes much of the growth-inhibitory effects of myelin. In contrast to the synapse studies, virtually all of the APC is located in the nuclei of these neurons, and the axon growth phenotype appears to be due to stabilization of Id2 and SnoN (Lasorella et al., 2006; Stegmuller et al., 2006).

Here, we identify a zebrafish mutant for *emi1* that ceases mitosis at the beginning of gastrulation. Using this mutant, we find that normal cell cycle progression is not required for segmentation clock function, but rather that mitosis is a modest source of noise for the

Department of Molecular, Cellular and Developmental Biology, Yale University, New Haven, CT 06520, USA.

*Author for correspondence (e-mail: scott.holley@yale.edu)

Accepted 25 April 2008

clock. Finally, we show that the cell cycle defect leads to hyper-epithelialization of the somites after the initiation of morphological segmentation.

MATERIALS AND METHODS

Zebrafish breeding, mapping and cloning

Breeding and meiotic mapping followed standard protocols (Geisler, 2002; Nüsslein-Volhard and Dahm, 2002). The coding sequence of *emi1* (GenBank NM_001003869) was isolated via RT-PCR and cloned into pCS2+. This clone was used to generate sense mRNA using the Ambion SP6 mMessage Machine kit, and an antisense riboprobe using the Roche digoxigenin-labeling mix. For allele sequencing, we used an *emi1* template from two independently derived *tiy121* RT-PCRs. Wild-type embryos were injected with 0.5 mM *emi1* morpholino targeting the splice donor of the second intron (5′-TGATTGTCGTTTCACCTCATCATCT-3′).

Immunohistochemistry, in situ hybridization

Fibronectin, phalloidin, S58 staining (Jülich et al., 2005a), and fluorescent in situ hybridization with β-catenin immunohistochemistry (Jülich et al., 2005b), were performed as previously described. All in situ hybridizations were performed with digoxigenin-labeled riboprobes. *her1* and *deltaC* antisense probes were made from plasmid clones, as previously described (Holley et al., 2000; Holley et al., 2002). The *tbx18*, *mesogenin*, *mespb* and *ripply1* coding sequences were isolated via RT-PCR and subjected to an additional round of PCR in which a T7 promoter was added in the antisense orientation. Antisense riboprobes were then created using T7 RNA polymerase (NEB). Integrin α5-GFP (Jülich et al., 2005a) and YFP-Emi1 were visualized with rabbit anti-GFP (1:1000, Invitrogen) and anti-rabbit Alexa 488 (1:200, Invitrogen). Goat anti-EphrinB2 (1:500, R&D Systems) was paired with anti-goat Alexa 647 (1:200, Invitrogen). Rabbit anti-Phospho-Histone H3 (PHH3) antibody (1:1000, Sigma) was used with goat anti-rabbit-HRP (1:400, Invitrogen) and Fluorescein TSA (Perkin Elmer).

We analyzed *her1* expression in *emi1* mutant and sibling embryos injected with translation-blocking morpholinos against either *deltaC* or *deltaD* (Holley et al., 2002). Three independent trials were performed with embryos derived from different parents and injected on different days. *deltaC* morpholino-injected and *deltaD* morpholino-injected embryos were fixed in 4% paraformaldehyde (PFA) at the ~2-somite and ~5-somite stages, respectively. Embryos were co-stained for *her1* expression with NBT/BCIP and for PHH3 by immunofluorescence. Absence of PHH3 staining was used to sort *emi1*$^{-/-}$ from sibling embryos.

Drug treatment and BrdU labeling

Embryos were incubated in 150 μM aphidicolin and 20 mM hydroxyurea (Sigma) in 4% DMSO, from the germ ring/early shield stage until fixation (Harris and Hartenstein, 1991; Lyons et al., 2005). Drug treatment at this stage blocked mitosis by the late shield stage, mimicking the onset of the *emi1*$^{-/-}$ phenotype. To assay for DNA synthesis, 10 mM BrdU was injected into the yolk just after the shield stage, at the 1-somite stage or at the 8-somite stage. Embryos were fixed in 4% PFA at the 14- to 15-somite stage. BrdU incorporation was visualized using a mouse anti-BrdU antibody (1:200, Sigma) and an Alexa 647-labeled goat anti-mouse antibody (1:200, Invitrogen). Embryos injected at each stage showed BrdU incorporation, indicating that endoreplication occurs continuously during late gastrulation and trunk segmentation in *emi1* mutants.

RESULTS AND DISCUSSION

We identified a zebrafish mutant, *tiy121*, which exhibits a mitotic block (Fig. 1A-D). By the shield stage, mutant embryos cease all mitosis, as visualized by immunostaining for phosphorylated Histone H3. Despite the mitotic arrest, mutant embryos undergo gastrulation and axis elongation (Fig. 1E,F). Measurement of the distance from the otic vesicle to the tip of the tail indicates that *tiy121* embryos (n=15) are on average 22% (s.d. ±3.2%) shorter than their wild-type siblings (n=17). After the mitotic block, mutant embryos continue endoreplication, as indicated by BrdU labeling (Fig. 1G,H). *tiy121* embryos ultimately develop a pericardial edema and extensive necrosis in the head, and die 2-3 days post-fertilization. The relatively normal progression of early development in *tiy121* embryos parallels the finding that early *Xenopus* development is unperturbed by the chemical inhibition of mitosis (Cooke, 1973; Harris and Hartenstein, 1991; Rollins and Andrews, 1991).

We mapped *tiy121*, via meiotic recombination, to chromosome 13 between the simple sequence length polymorphisms (SSLP) z24268 and z55656, near a zebrafish homolog of *early mitotic inhibitor 1* (*emi1*) (Fig. 2A). Determination of the *emi1* coding sequence in the single mutant allele revealed a premature stop codon that truncates the protein prior to the F-box domain, which is likely to create an amorphic allele (Fig. 2B). Injection of a splice-blocking morpholino against *emi1* recapitulates the mitotic defect through gastrulation. However, the antisense inhibition declines by the tailbud stages, and mitosis is normal by the 5-somite stage (Fig. 2C). In morpholino-injected embryos, phosphorylated Histone H3 staining (PHH3) was absent (89%) or reduced (9%) at the shield stage (n=101), was reduced in 79% of embryos at the tailbud stage (n=39), and was indistinguishable from controls at the 5-somite stage (n=37). Injection of in vitro synthesized mRNA for *YFP-emi1* rescues the mitotic defect through gastrulation, but the rescue declines by the tailbud stage and is absent by the 18-somite stage

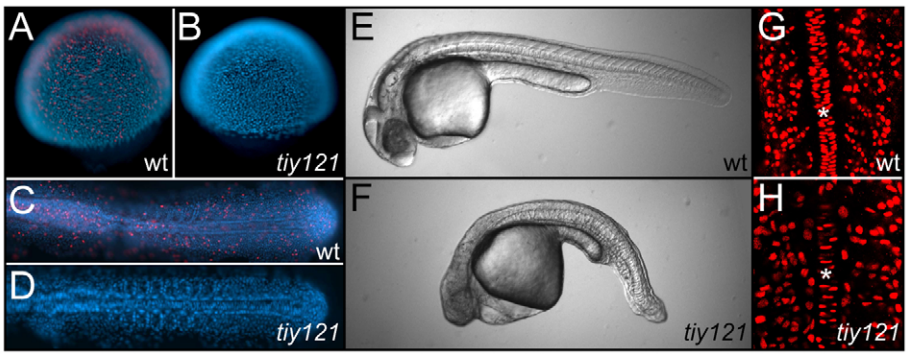

Fig. 1. *tiy121* mutants have a cell cycle defect. (**A-D**) Phosphorylated Histone H3 staining (PHH3, red) marks mitotic cells in wild-type embryos at the shield (A) and 10-somite stage (C). No mitotic nuclei are seen in *tiy121* embryos at the shield (B) or 10-somite stage (D). Nuclei are stained with DAPI (blue). (**E**,**F**) Wild-type (E) and *tiy121*$^{-/-}$ (F) embryos at 30 hpf. (**G**,**H**) BrdU labeling (red) in the trunks of wild type (G) and *tiy121*$^{-/-}$ (H) at the 14-somite stage. Asterisks label the notochord. BrdU was injected into the yolk at the 8-somite stage. In C-F, anterior is left; in G and H, anterior is up.

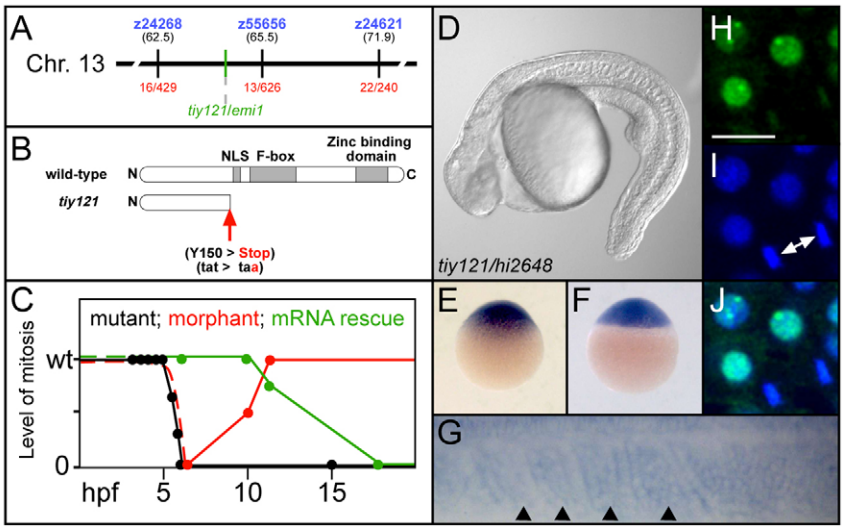

Fig. 2. *tiy121* is an *emi1* mutant. (**A**) The chromosomal location of *tiy121/emi1*. (**B**) *tiy121* is a premature stop codon in *emi1*. NLS, nuclear localization signal. (**C**) Graph of the levels of mitosis in *tiy121*, *emi1* morphants, and *tiy121* embryos rescued by injection of *emi1* mRNA. The level of mitosis, graphed along an arbitrary scale, was wild-type (wt) or reduced to some degree, or mitosis was absent. Morphants and mRNA-injected embryos develop normally prior to the shield stage, thus we infer that the initial level of mitosis is normal without examining PHH3 (dashed lines). hpf, hours post fertilization. (**D**) *tiy121* and *hi2648*, an insertional allele of *emi1*, do not complement. (**E-G**) Expression of *emi1* mRNA (E) at the one-cell stage, (F) at the sphere stage, and (G) in the most recently formed somites (arrowheads) and anterior PSM of a 12-somite stage embryo. Anterior is left in G. (**H**) YFP-Emi1 immunofluorescence. (**I**) DAPI stained nuclei. (**J**) Overlay of H and I. Arrows indicate a cell completing mitosis. Scale bar in H: 20 μm for H-J.

(Fig. 2C). *YFP-emi1* mRNA (5 ng/μl) was injected into clutches from *tiy121*$^{+/-}$ parents. Normal PHH3 was seen in 99% (*n*=75) and 98% (*n*=141) of embryos at the shield and tailbud stage, respectively. By the 5-somite stage, 16% (*n*=110) showed reduced PHH3, and at the 18-somite stage, 27% (*n*=153) showed no PPH3. *tiy121* fails to complement *hi2648*, a hypomorphic, retroviral allele of *emi1* (Fig. 2D) (Amsterdam et al., 2004). Together, these data indicate that the *tiy121* phenotype is due to perturbation of *emi1*.

emi1 mRNA is maternally deposited (Fig. 2E), and later ubiquitously expressed in the blastula and gastrula stages (Fig. 2F). Emi1-YFP protein localizes to the nucleus but is diminished in cells undergoing mitosis (Fig. 2H-J). During segmentation, *emi1* is broadly expressed, including within the somites (Fig. 2G).

Although *tiy121* embryos are short, the mutant phenotype indicates that cell proliferation is not absolutely required for trunk and tail extension. However, the mutants display irregularly sized and partially fused somites and myotomes (Fig. 3A-D; see also Fig. S1 in the supplementary material). The segmentation clock creates oscillations in transcription that manifest as stripes of expression sweeping through the cells of the PSM in a wave-like fashion. We examined the expression of three oscillating genes, *her1*, *her7* and *deltaC*, at the 3-, 8- and 15-somite stage and found no appreciable defect in their expression in *emi1*$^{-/-}$ (Fig. 3E-J; data not shown). Note that, at the 8- and 15-somite stage, the tailbud of *emi1*$^{-/-}$ embryos is smaller than normal (compare Fig. 3F and G to 3I and J, respectively). This decrease is reflected in the reduction of the domain of *mesogenin* expression (see Fig. S1 in the supplementary material). Although *emi1* mutants undergo mitosis at the beginning of gastrulation when oscillations are first seen (Riedel-Kruse et al., 2007), our data indicate that continued oscillation of the segmentation clock is not dependent upon the cell cycle.

In contrast to models that link the cell cycle to the segmentation clock, it has been postulated that mitosis is actually a source of noise for the clock (Horikawa et al., 2006). To test this hypothesis, we examined the effect of inhibiting mitosis in embryos lacking either of the Notch ligands *deltaC* or *deltaD*. The *deltaC* and *deltaD* mutants form the first 3-5 and 7-9 somites, respectively, as the oscillating pattern of gene expression gradually breaks down, leading to the segmentation defect (Fig. 3K-N; see also Fig. S1 in the supplementary material) (Holley et al., 2000; Jiang et al., 2000; Jülich et al., 2005b; Oates et al., 2005a; van Eeden et al., 1996; van Eeden et al., 1998). This breakdown may be accelerated because of noise. Thus, if mitosis is a source of noise in the segmentation program, one would predict that the breakdown would decelerate in the absence of cell division. We assayed the expression of *her1* mRNA in *deltaD* or *deltaC* morpholino-injected embryos that were either wild type or mutant for *emi1* (Fig. 3N, Fig. S1 in the supplementary material). The difference between the mutants and siblings was not immediately apparent. However, upon careful categorization of the expression patterns, we found a subtle improvement in the integrity of the *her1* stripes in embryos lacking *emi1* compared with sibling embryos. For each trial, the more organized stripe patterns are biased towards the injected *emi1* mutants, and the two more disorganized expression categories are biased towards the injected siblings. In summary, these results are consistent with mitosis being a modest source of noise in the segmentation clock.

Further examination of the segmentation defect in *emi1*$^{-/-}$ embryos revealed profound abnormalities in somite morphology. Although *emi1*$^{-/-}$ somites initially contain internal mesenchymal cells, these cells leave the core of the somite and at least some integrate into the epithelial somite boundary (Fig. 4A,B,D,E). We have observed other cells migrating to the lateral surface of the paraxial mesoderm. The somite boundary cells then appear to elongate and meet in the middle of each segment, creating somites solely consisting of two rows of boundary cells (Fig. 4B,E,G,I). These hyper-epithelialized somites, having no internal mesenchyme and abnormally elongated epithelial border cells, often fuse to create irregularly sized segments. The nuclei

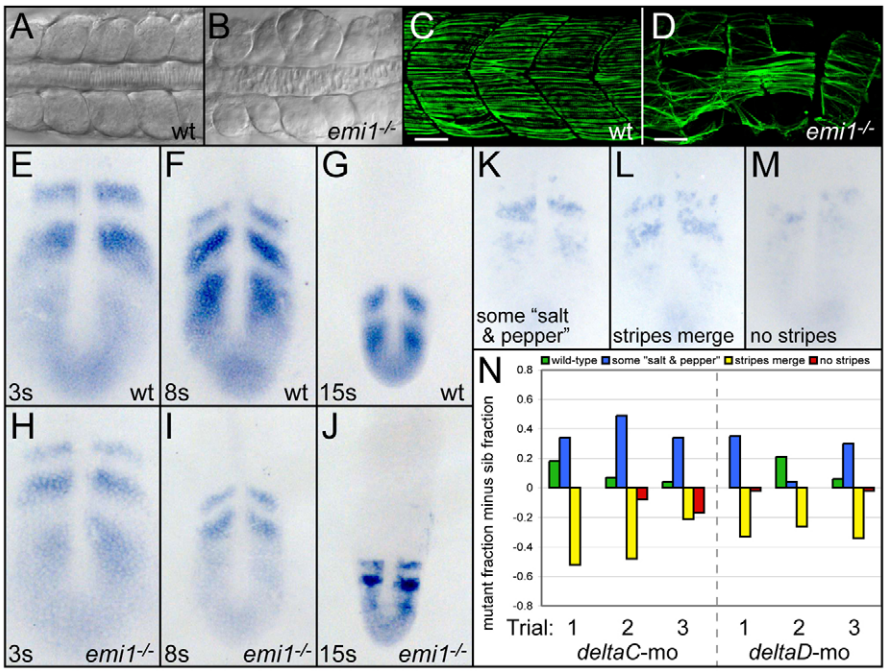

Fig. 3. Cell cycle progression is necessary for somitogenesis but not segmentation clock function. (**A**,**B**) Dorsal views of anterior trunk somites in wild-type (A) and *emi1*$^{-/-}$ (B) embryos at the 15-somite stage. (**C**,**D**) Posterior trunk myotomes of wild-type (C) and *emi1*$^{-/-}$ (D) embryos at 36 hpf, lateral views. Slow muscle fibers are labeled with S58 antibodies (green). Scale bars: 30 μm. (**E-J**) *her1* expression at the 3-, 8- and 15-somite stages in (E-G) wild-type and (H-J) *emi1*$^{-/-}$ embryos. (**K-N**) *her1* stripe integrity was examined in *emi1*$^{-/-}$ and sibling embryos injected with morpholinos against either *deltaC* or *deltaD*. *her1* expression was rated according to four categories representing increasing levels of disorganization: wild type; (K) stripes with some 'salt and pepper' expression; (L) stripes begin to merge; and (M) no stripes. (N) Distributions of gene expression patterns are displayed for three independent trials (*x*-axis). Within each gene expression category, the fraction of sibling embryos is subtracted from the fraction of mutant embryos. For example, the wild-type category in the first *deltaC* morpholino trial included 0.20 fraction of the mutant embryos (20%) and 0.02 fraction of the sibling embryos (2%), giving a graphed value of 0.18. In *deltaC* morpholino trials, the number of mutants and siblings assayed (mutant/siblings) were: 39/74, 27/79 and 16/57. For *deltaD* morpholino trials, the corresponding numbers were: 60/50, 28/74 and 49/90. Given the subjective nature of the expression classification, a second assayer performed an independent blind classification of the same embryos (see Fig. S1 in the supplementary material). Although the profiles of the distributions differ, the distinction between *emi1* and sibling embryos was consistent. In A-D, anterior is left. In E-M, anterior is up.

of the boundary cells show a basal localization, as does Integrin α5-GFP clustering (Fig. 4A,B). Fibronectin matrix is also assembled along the somite boundaries (Fig. 4F,G). This maintenance of border cell polarity distinguishes the *emi1*$^{-/-}$ phenotype from that of *integrin* α5 and *fibronectin1a* mutants (Jülich et al., 2005a; Koshida et al., 2005). Ephrin B2 is localized to the cortex of the somite cells, with slightly higher levels in the posterior somite cells, and this pattern appears largely intact in *emi1*$^{-/-}$ (Fig. 4H,I; see also Fig. S1 in the supplementary material). Expression of *mespb*, *ripply1* and *tbx18*, *myod* and *deltaC* is clearly segmental, although there is some aberrant expression of *deltaC* in the mutant embryos (Fig. 4J-M; Fig. S1 in the supplementary material). The segment polarity alterations observed in *emi1* mutants are slight in comparison to those defects seen in *fss* and the Notch pathway mutants, and seem unlikely to be the cause of the morphological phenotype.

The morphological analysis suggests that the polarity of the somite boundary cells is maintained. In addition, the somite phenotype does not seem to follow from a defect in anteroposterior patterning of the somites. Rather, it appears that the somites in *emi1*$^{-/-}$ mutant embryos are hyper-epithelialized. The hyper-epithelialization could be due to elevated APC activity, which may affect the stability of proteins involved in regulating cell morphology independently of the cell cycle (Juo and Kaplan, 2004; Konishi et al., 2004; Lasorella et al., 2006; Stegmuller et al., 2006; van Roessel et al., 2004). To test this hypothesis, we blocked mitosis using a combination of hydroxyurea and aphidicolin (Harris and Hartenstein, 1991; Lyons et al., 2005). Addition of the compounds at the germ ring/early shield stage blocked all mitosis by the late shield stage and resulted in embryos lacking internal mesenchymal cells in their somites, strongly phenocopying *emi1*$^{-/-}$ (Fig. 4C; see also Fig. S1 in the supplementary material). These data suggest that the segmentation defect in *emi1*$^{-/-}$ mutant embryos is primarily due to the lack of normal cell cycle progression and not to a cell cycle-independent function of *emi1* or APC. Note that in both mutant and drug-treated embryos, the cells and nuclei are larger than in wild type (Fig. 4). The increase in cell size, along with the decrease in cell number, might also be causally linked to the somite morphogenesis defect.

The mitotic defect in *emi1*$^{-/-}$ embryos arises after the midblastula transition (MBT). MBT initiates during the tenth cell cycle [3 hours post-fertilization (hpf)], when divisions become asynchronous and zygotic transcription commences (Kane, 1999; Kane and Kimmel, 1993). During cycles 11 and 12, the blastula forms three domains, the extra-embryonic yolk syncytial layer and enveloping layer, and the deep cells that give rise to the embryo proper (Kane, 1999). At 5.5 hpf, gastrulation starts, as most of the deep cells are in cell cycle 14 (Kane, 1999; Kane et al., 1992). *emi1*$^{-/-}$ embryos cease cell division around this time. In wild-type embryos, the cell cycle lengthens during this period, with the thirteenth, fourteenth, fifteenth

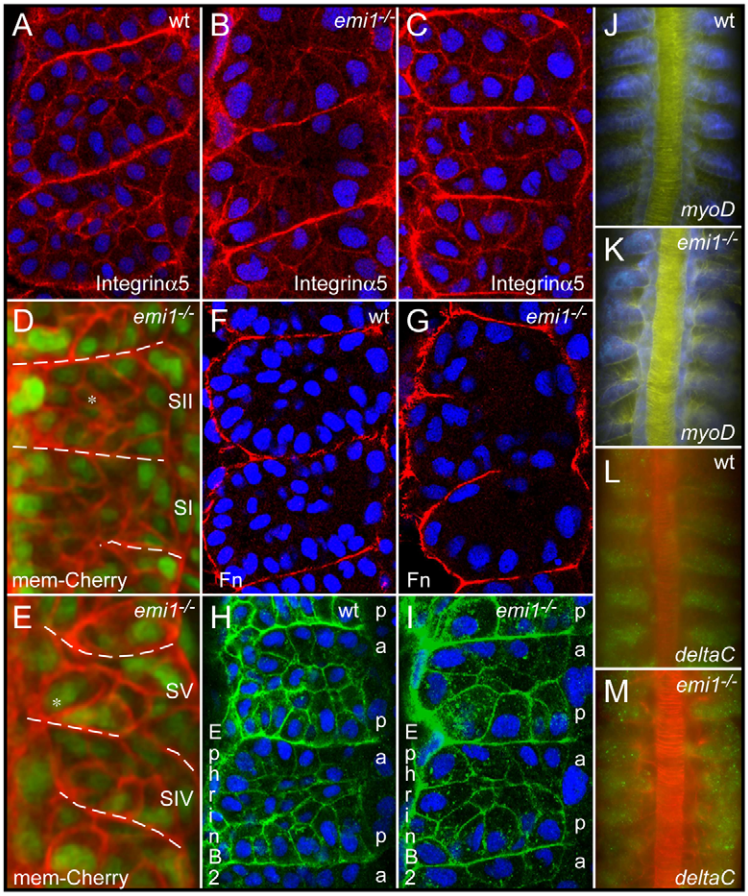

Fig. 4. Cell cycle inhibition leads to somite hyperepithelialization. (**A-C**) Integrin α5-GFP (red) labels the cell cortex and clusters along somite borders in (A) wild-type (wt), (B) *emi1*$^{-/-}$ and (C) aphidicolin-hydroxyurea-treated embryos. Embryos were at the 12-somite stage. Somites 2-4, 3-5 and 3-5 are shown, respectively. (**D**,**E**) 12-somite-stage *emi1*$^{-/-}$ embryo labeled with membrane-localized cherry (red) to visualize the cell cortex. The same somites at the beginning (SI and SII) and end (SIV and SV, respectively) of a timelapse are shown. The somite borders are indicated by dashed lines. Somites initially have internal mesenchymal cells, but after three somite cycles have passed, the internal mesenchymal cells (asterisk in D) have moved to the surface of the somite (asterisk in E). (**F**,**G**) Fibronectin (Fn) matrix (red) forms along the borders in (F) wild type and (G) *emi1*$^{-/-}$. Embryos were at the 12-somite stage. Somites 6-7 and 3-5 are pictured. (**H**,**I**) Ephrin B2 expression (green) shows a graded, segmental distribution in (H) wild type and (I) *emi1*$^{-/-}$. The lateral membranes of the posterior (p) somite border cells show higher levels of Ephrin B2 than do the lateral membranes of anterior (a) border cells. Embryos were at the 12-somite stage. Shown are somites 5-6 and 4-5. (**J**,**K**) Segmental expression of *myod* (blue) in (J) wild type, somites 3-8, and (K) *emi1*$^{-/-}$, somites 4-9, in 10-somite-stage embryos. (**L**,**M**) Expression of *deltaC* (green) in (L) wild type, somites 4-9, is aberrant, but segmental in (M) *emi1*$^{-/-}$, somites 4-9, in 10-somite-stage embryos. Nuclei are labeled with DAPI (blue) in A-C,F-I. In D and E, nuclei are labeled with nuclear-GFP (green). β-catenin labels the cell cortex in J,K (yellow) and L,M (red). In all panels, anterior is up.

and sixteenth cycles averaging 54, 78, 151 and 240 minutes, respectively. During segmentation, most cells are in either cell cycle 16 or 17 (Kane, 1999). The mild elongation defect in *emi1*$^{-/-}$ is likely to be due to the fact that mitosis is normally not a great contributor to axial growth during the segmentation period. This conclusion was also reached by examining the elongation of clonal strings of cells in the CNS: the exponential lengthening of the string suggested that it was largely due to cell intercalation and not cell division (Kimmel et al., 1994). The relatively normal differentiation in *emi1*$^{-/-}$ embryos can be explained by the fact that many cells undergo a terminal differentiation during cell cycle 15, 8-10 hpf, and a major wave of differentiation occurs during cycle 16 (Kane, 1999; Kimmel et al., 1994; Kimmel and Warga, 1987). Thus, for many cell lineages, the mitotic defect in *emi1* embryos does not reduce dramatically the number of cell cycles that these cells would normally undergo.

The cell cycle could in principle serve as a clock to regulate developmental timing (Johnson and Day, 2000). Experiments in ascidians have suggested that the timing of myogenesis may depend upon the number of cycles of DNA synthesis that a myogenic progenitor experiences (Satoh, 1987). However, previous cell labeling experiments indicate that zebrafish myofiber differentiation is not regulated by such a cell cycle-counting mechanism (Kimmel and Warga, 1987). Similarly, the expression of differentiation markers in the *C. elegans* gut occurs independently of cell cycle counting (Edgar and McGhee, 1988). The segmentation clock has been suggested to be linked to the cell cycle oscillator. Reiterated segmentation defects are seen in chick embryos after treatment with cell-cycle inhibitors, and the periodicity of this defect is equal to the cell cycle length at that stage of development (Primmett et al., 1989). Similar periodic defects were seen after a single heat shock (Primmett et al., 1988). More recently, this cell cycle model has been formalized mathematically (Collier et al., 2000; McInerney et al., 2004). In the zebrafish, a single heat shock can produce reiterated segmentation defects, but the periodicity of the defect does not correlate with the length of the cell cycle during segmentation (Roy et al., 1999). Additionally, there is no organized pattern of cell proliferation in the zebrafish tailbud (Kanki and Ho, 1997). Our analysis of the *emi1* mutant indicates that cell cycle progression is not required for zebrafish segmentation clock function. Conversely, our data are consistent with the hypothesis that mitosis is a modest source of noise for the segmentation clock (Horikawa et al., 2006).

We thank Hiroyuki Takeda and members of the lab for comments on the manuscript. The *tiy121* mutant was isolated in the Tübingen 2000 Screen, and we acknowledge all participants of the consortium: F. Van Bebber, E. Busch-Nentwich, R. Dahm, O. Frank, H.-G. Fronhöfer, H. Geiger, D. Gilmour, S. Holley, J. Hooge, D. Jülich, H. Knaut, F. Maderspacher, H.-M. Maischein, C. Neumann, C. Nüsslein-Volhard, H. Roehl, U. Schönberger, C. Seiler, S. Sidi, M. Sonawane, A. Wehner, P. Erker, H. Habeck, U. Hagner, C. E. Hennen Kaps, A. Kirchner, T. Koblizek, U. Langheinrich, C. Loeschke, C. Metzger, R. Nordin, J. Odenthal, M. Pezzuti, K. Schlombs, J. de Santana-Stamm, T. Trowe, G. Vacun, B. Walderich, A. Walker and C. Weiler. We thank Nancy Hopkins for the *hi2648* allele. We thank Joseph Wolenski for assistance with the confocal microscopy. This work was supported by the March of Dimes Foundation, research grant number 1-FY07-424, and the NICHD, R01 HD045738.

Supplementary material

Supplementary material for this article is available at
http://dev.biologists.org/cgi/content/full/135/12/2065/DC1

References

Amsterdam, A., Nissen, R. M., Sun, Z., Swindell, E. C., Farrington, S. and Hopkins, N. (2004). Identification of 315 genes essential for early zebrafish development. *Proc. Natl. Acad. Sci. USA* **101**, 12792-12797.

Aulehla, A., Wehrle, C., Brand-Saberi, B., Kemler, R., Gossler, A., Kanzler, B. and Herrmann, B. G. (2003). Wnt3a plays a major role in the segmentation clock controling somitogenesis. *Dev. Cell* **4**, 395-406.
Barrios, A., Poole, R. J., Durbin, L., Brennan, C., Holder, N. and Wilson, S. W. (2003). Eph/Ephrin signaling regulates the mesenchymal-to-epithelial transition of the paraxial mesoderm during somite morphogenesis. *Curr. Biol.* **13**, 1571-1582.
Collier, J. R., McInerney, D., Schnell, S., Maini, P. K., Gavaghan, D. J., Houston, P. and Stern, C. D. (2000). A cell cycle model for somitogenesis: mathematical formulation and numerical simulation. *J. Theor. Biol.* **207**, 305-316.
Cooke, J. (1973). Morphogenesis and regulation in spite of continued mitotic inhibition in Xenopus embryos. *Nature* **242**, 55-57.
Dale, J. K., Malapert, P., Chal, J., Vilhais-Neto, G., Maroto, M., Johnson, T., Jayasinghe, S., Trainor, P., Herrmann, B. and Pourquie, O. (2006). Oscillations of the snail genes in the presomitic mesoderm coordinate segmental patterning and morphogenesis in vertebrate somitogenesis. *Dev. Cell* **10**, 355-366.
Dequeant, M. L., Glynn, E., Gaudenz, K., Wahl, M., Chen, J., Mushegian, A. and Pourquie, O. (2006). A complex oscillating network of signaling genes underlies the mouse segmentation clock. *Science* **314**, 1595-1598.
Durbin, L., Brennan, C., Shiomi, K., Cooke, J., Barrios, A., Shanmugalingam, S., Guthrie, B., Lindberg, R. and Holder, N. (1998). Eph signaling is required for segmentation and differentiation of the somites. *Genes Dev.* **12**, 3096-3109.
Durbin, L., Sordino, P., Barrios, A., Gering, M., Thisse, C., Thisse, B., Brennan, C., Green, A., Wilson, S. and Holder, N. (2000). Anteriorposterior patterning is required within segments for somite boundary formation in developing zebrafish. *Development* **127**, 1703-1713.
Edgar, L. G. and McGhee, J. D. (1988). DNA synthesis and the control of embryonic gene expression in C. elegans. *Cell* **53**, 589-599.
Geisler, R. (2002). Mapping and cloning. In *Zebrafish* (ed. C. Nusslein-Volhard and R. Dahm), pp. 175-212. Oxford: Oxford University Press.
Georges-Labouesse, E. N., George, E. L., Rayburn, H. and Hynes, R. O. (1996). Mesodermal development in mouse embryos mutant for fibronectin. *Dev. Dyn.* **207**, 145-156.
Goh, K. L., Yang, J. T. and Hynes, R. O. (1997). Mesodermal defects and cranial neural crest apoptosis in alpha5 integrin-null embryos. *Development* **124**, 4309-4319.
Harris, W. A. and Hartenstein, V. (1991). Neuronal determination without cell division in Xenopus embryos. *Neuron* **6**, 499-515.
Holley, S. A. (2007). The genetics and embryology of zebrafish metamerism. *Dev. Dyn.* **236**, 1422-1449.
Holley, S. A., Geisler, R. and Nüsslein-Volhard, C. (2000). Control of *her1* expression during zebrafish somitogenesis by a *Delta*-dependent oscillator and an independent wave-front activity. *Genes Dev.* **14**, 1678-1690.
Holley, S. A., Jülich, D., Rauch, G. J., Geisler, R. and Nüsslein-Volhard, C. (2002). her1 and the notch pathway function within the oscillator mechanism that regulates zebrafish somitogenesis. *Development* **129**, 1175-1183.
Horikawa, K., Ishimatsu, K., Yoshimoto, E., Kondo, S. and Takeda, H. (2006). Noise-resistant and synchronized oscillation of the segmentation clock. *Nature* **441**, 719-723.
Jiang, Y.-J., Aerne, B. L., Smithers, L., Haddon, C., Ish-Horowicz, D. and Lewis, J. (2000). Notch signaling and the synchronization of the somite segmentation clock. *Nature* **408**, 475-479.
Johnson, M. H. and Day, M. L. (2000). Egg timers: how is developmental time measured in the early vertebrate embryo? *BioEssays* **22**, 57-63.
Jülich, D., Geisler, R. and Holley, S. A. (2005a). Integrinα5 and Delta/Notch signalling have complementary spatiotemporal requirements during zebrafish somitogenesis. *Dev. Cell* **8**, 575-586.
Jülich, D., Lim, C.-H., Round, J., Nicolaije, C., Davies, A., Schroeder, J., Geisler, R., Consortium, T. S., Lewis, J., Jiang, Y.-J. et al. (2005b). beamter/deltaC and the role of Notch ligands in the zebrafish somite segmentation, hindbrain neurogenesis and hypochord differentiation. *Dev. Biol.* **286**, 391-404.
Juo, P. and Kaplan, J. M. (2004). The anaphase-promoting complex regulates the abundance of GLR-1 glutamate receptors in the ventral nerve cord of C. elegans. *Curr. Biol.* **14**, 2057-2062.
Kane, D. A. (1999). Cell cycles and development in the embryonic zebrafish. *Methods Cell Biol.* **59**, 11-26.
Kane, D. A. and Kimmel, C. B. (1993). The zebrafish midblastula transition. *Development* **119**, 447-456.
Kane, D. A., Warga, R. M. and Kimmel, C. B. (1992). Mitotic domains in the early embryo of the zebrafish. *Nature* **360**, 735-737.
Kanki, J. P. and Ho, R. K. (1997). The development of the posterior body in zebrafish. *Development* **124**, 881-893.
Kimmel, C. B. and Warga, R. W. (1987). Cell lineages generating axial muscle in the zebrafish embryo. *Nature* **327**, 234-237.
Kimmel, C. B., Warga, R. M. and Kane, D. A. (1994). Cell cycles and clonal strings during formation of the zebrafish central nervous system. *Development* **120**, 265-276.
Konishi, Y., Stegmuller, J., Matsuda, T., Bonni, S. and Bonni, A. (2004). Cdh1-APC controls axonal growth and patterning in the mammalian brain. *Science* **303**, 1026-1030.
Koshida, S., Kishimoto, Y., Ustumi, H., Shimizu, T., Furutani-Seiki, M., Kondoh, H. and Takada, S. (2005). Integrinalpha5-dependent fibronectin accumulation for maintenance of somite boundaries in zebrafish embryos. *Dev. Cell* **8**, 587-598.
Kragtorp, K. A. and Miller, J. R. (2006). Regulation of somitogenesis by Ena/VASP proteins and FAK during Xenopus development. *Development* **133**, 685-695.
Kragtorp, K. A. and Miller, J. R. (2007). Integrin alpha5 is required for somite rotation and boundary formation in Xenopus. *Dev. Dyn.* **236**, 2713-2720.
Lasorella, A., Stegmuller, J., Guardavaccaro, D., Liu, G., Carro, M. S., Rothschild, G., de la Torre-Ubieta, L., Pagano, M., Bonni, A. and Iavarone, A. (2006). Degradation of Id2 by the anaphase-promoting complex couples cell cycle exit and axonal growth. *Nature* **442**, 471-474.
Lyons, D. A., Pogoda, H. M., Voas, M. G., Woods, I. G., Diamond, B., Nix, R., Arana, N., Jacobs, J. and Talbot, W. S. (2005). erbb3 and erbb2 are essential for schwann cell migration and myelination in zebrafish. *Curr. Biol.* **15**, 513-524.
McInerney, D., Schnell, S., Baker, R. E. and Maini, P. K. (2004). A mathematical formulation for the cell-cycle model in somitogenesis: analysis, parameter constraints and numerical solutions. *Math. Med. Biol.* **21**, 85-113.
Nakajima, Y., Morimoto, M., Takahashi, Y., Koseki, H. and Saga, Y. (2006). Identification of Epha4 enhancer required for segmental expression and the regulation by Mesp2. *Development* **133**, 2517-2525.
Nakaya, Y., Kuroda, S., Katagiri, Y. T., Kaibuchi, K. and Takahashi, Y. (2004). Mesenchymal-epithelial transition during somitic segmentation is regulated by differential roles of Cdc42 and Rac1. *Dev. Cell* **7**, 425-438.
Nikaido, M., Kawakami, A., Sawada, A., Furutani-Seiki, M., Takeda, H. and Araki, K. (2002). Tbx24, encoding a T-box protein, is mutated in the zebrafish somite-segmentation mutant fused somites. *Nat. Genet.* **31**, 195-199.
Niwa, Y., Masamizu, Y., Liu, T., Nakayama, R., Deng, C. X. and Kageyama, R. (2007). The initiation and propagation of Hes7 oscillation are cooperatively regulated by Fgf and notch signaling in the somite segmentation clock. *Dev. Cell* **13**, 298-304.
Nüsslein-Volhard, C. and Dahm, R. (2002). *Zebrafish: A Practical Approach* (ed. B. D. Hames). Oxford: Oxford University Press.
Oates, A. C., Mueller, C. and Ho, R. K. (2005a). Cooperative function of deltaC and her7 in anterior segment formation. *Dev. Biol.* **280**, 133-149.
Oates, A. C., Rohde, L. A. and Ho, R. K. (2005b). Generation of segment polarity in the paraxial mesoderm of the zebrafish through a T-box-dependent inductive event. *Dev. Biol.* **283**, 204-214.
Pourquié, O. (2003). The segmentation clock: converting embryonic time into spatial pattern. *Science* **301**, 328-330.
Primmett, D. R., Stern, C. D. and Keynes, R. J. (1988). Heat shock causes repeated segmental anomalies in the chick embryo. *Development* **104**, 331-339.
Primmett, D. R., Norris, W. E., Carlson, G. J., Keynes, R. J. and Stern, C. D. (1989). Periodic segmental anomalies induced by heat shock in the chick embryo are associated with the cell cycle. *Development* **105**, 119-1130.
Reimann, J. D., Freed, E., Hsu, J. Y., Kramer, E. R., Peters, J. M. and Jackson, P. K. (2001). Emi1 is a mitotic regulator that interacts with Cdc20 and inhibits the anaphase promoting complex. *Cell* **105**, 645-655.
Riedel-Kruse, I. H., Muller, C. and Oates, A. C. (2007). Synchrony dynamics during initiation, failure, and rescue of the segmentation clock. *Science* **317**, 1911-1915.
Rollins, M. B. and Andrews, M. T. (1991). Morphogenesis and regulated gene activity are independent of DNA replication in Xenopus embryos. *Development* **112**, 559-569.
Roy, M. N., Prince, V. E. and Ho, R. K. (1999). Heat shock produces periodic somitic disturbances in the zebrafish embryo. *Mech. Dev.* **85**, 27-34.
Satoh, N. (1987). Towards a molecular understanding of differentiation mechanisms in ascidian embryos. *BioEssays* **7**, 51-56.
Stegmuller, J., Konishi, Y., Huynh, M. A., Yuan, Z., Dibacco, S. and Bonni, A. (2006). Cell-intrinsic regulation of axonal morphogenesis by the Cdh1-APC target SnoN. *Neuron* **50**, 389-400.
van Eeden, F. J. M., Granato, M., Schach, U., Brand, M., Furutani-Seiki, M., Haffter, P., Hammerschmidt, M., Heisenberg, C.-P., Jiang, Y.-J., Kane, D. A. et al. (1996). Mutations affecting somite formation and patterning in the zebrafish *Danio rerio*. *Development* **123**, 153-164.
van Eeden, F. J. M., Holley, S. A., Haffter, P. and Nüsslein-Volhard, C. (1998). Zebrafish segmentation and pair-rule patterning. *Dev. Genet.* **23**, 65-76.
van Roessel, P., Elliott, D. A., Robinson, I. M., Prokop, A. and Brand, A. H. (2004). Independent regulation of synaptic size and activity by the anaphase-promoting complex. *Cell* **119**, 707-718.
Wahl, M. B., Deng, C., Lewandoski, M. and Pourquie, O. (2007). FGF signaling acts upstream of the NOTCH and WNT signaling pathways to control segmentation clock oscillations in mouse somitogenesis. *Development* **134**, 4033-4041.
Yang, J. T., Rayburn, H. and Hynes, R. O. (1993). Embryonic mesodermal defects in alpha 5 integrin-deficient mice. *Development* **119**, 1093-1105.